DMD Fast Forward. Published on August 15, 2018 as DOI: 10.1124/dmd.118.083584
This article has not been copyedited and formatted. The final version may differ from this version.

Title Page

Pheophorbide A: Fluorescent Bcrp substrate to measure oral drug-drug interactions in real time *in vivo*

Kazuto Yasuda, Samit Ganguly, and Erin G. Schuetz

Department of Pharmaceutical Sciences, St Jude Children's Research Hospital, Memphis, TN, (K.Y., S.G., E.G.S.), Cancer & Developmental Biology Track, University of Tennessee Health Science Center, Memphis, TN (S.G.)

Downloaded from dmd.aspetjournals.org at ASPET Journals on April 23, 2024

DMD Fast Forward. Published on August 15, 2018 as DOI: 10.1124/dmd.118.083584
This article has not been copyedited and formatted. The final version may differ from this version.

Running Title Page

Running title: Pheophorbide A: a *in vivo* probe of ABCG2 function/inhibition

Co-Corresponding Authors:
Erin G. Schuetz, PhD
Department of Pharmaceutical Sciences
St Jude Children's Research Hospital
262 Danny Thomas Place
Memphis, TN 38105, USA.
Phone + 1 901 595 2205
Email: erin.schuetz@stjude.org

Samit Ganguly, PhD
Department of Pharmaceutical Sciences
St Jude Children's Research Hospital
Email: samit@email.unc.edu

Number of Text Pages:

Number of Tables: 1

Number of Figures: 5

Number of References: 39

Number of words in Abstract: 250

Number of words in Introduction: 633

Number of words in Discussion: 1416

Number of Supplemental Figures: 4

Abbreviations: PhA, pheophorbide A; NIR, near-infrared; DDI, drug-drug interaction; LPB, lapatinib; CCM, curcumin; ECD, elacridar; PPZ, pantoprazole; DSB, dasatinib; SFB, sorafenib ; ITC, International Transporter Consortium; FDA, Food and Drug Administration; IVIS, in vivo imaging system; FTC, fumitremorgin C; AFF, alfalfa-free; CLPa, chlorophyll; PPIX, protoporphyrin IX.

Downloaded from dmd.aspetjournals.org at ASPET Journals on April 23, 2024

DMD Fast Forward. Published on August 15, 2018 as DOI: 10.1124/dmd.118.083584
This article has not been copyedited and formatted. The final version may differ from this version.

ABSTRACT

We investigated whether pheophorbide A (PhA) could serve as a selective BCRP substrate (victim) to screen *in vivo* using fluorescent live animal imaging for transporter-mediated interactions with orally administered inhibitors (perpetrators), and whether that could be coupled with serum sampling to measure PhA's systemic concentration with a fast-throughput *in vitro* fluorescent assay. PhA is a breakdown product of chlorophyll and is highly fluorescent in the near infrared (NIR) spectrum. Whole body NIR fluorescence was greater in the Bcrp KO compared to WT mice fed a regular diet containing chlorophyll and PhA, with fluorescence in WT mice confined to the intestine. PhA intestinal enterocyte fluorescence, after removing lumen contents, was greater in Bcrp KO vs. WT mice due to PhA enterocyte absorption and lack of PhA efflux by Bcrp. This difference was eliminated by maintaining the mice on an alfalfa (chlorophyll/PhA) free diet. The $AUC_{FL\ 0\text{-}6h}$ of orally administrated PhA was 3.5-times greater in the Bcrp KO compared to WT mice, and the PhA serum concentration was 50-fold higher in KO mice. Pre-treatment with known BCRP inhibitors lapatinib, curcumin, elacridar, pantoprazole, and sorafenib, at clinically relevant doses, significantly increased PhA $AUC_{FL\ 0\text{-}6h}$ by 2.4-, 2.3-, 2.2-, 1.5- and 1.4-fold, respectively, while PhA serum $AUC_{Serum\ 0\text{-}6h}$ increased by 13.8-, 7.8-, 5.2-, 2.02-, and 1.45-fold, respectively, and corresponded to their hierarchy as *in vitro* BCRP inhibitors. Our results demonstrate that live animal imaging utilizing PhA can be used to identify BCRP inhibitors and to assess the potential for BCRP mediated clinical drug-drug interactions.

Downloaded from dmd.aspetjournals.org at ASPET Journals on April 23, 2024

DMD Fast Forward. Published on August 15, 2018 as DOI: 10.1124/dmd.118.083584
This article has not been copyedited and formatted. The final version may differ from this version.

INTRODUCTION

The xenobiotic efflux transporter, breast cancer resistance protein (BCRP), encoded by *ABCG2*, is well characterized for its effect on the pharmacokinetics and pharmacodynamics of multiple drugs (Schwabedissen and Kroemer, 2011). Intestinal BCRP/ABCG2 has a significant effect limiting the oral bioavailability of its substrates (Roberts et al., 2016) that include drugs such as the nucleoside reverse-transcriptase inhibitor anti-retroviral drugs, calcium channel blockers, HMG-CoA reductase inhibitors, and topoisomerase I inhibitors, but also includes endogenous dietary substances such as the chlorophyll metabolite pheophorbide A (PhA) (Krishnamurthy and Schuetz, 2006; Robey et al., 2009; Schwabedissen and Kroemer, 2011). Moreover, multiple clinically used drugs, such as the tyrosine kinase inhibitor lapatinib, Human Immunodeficiency Virus protease inhibitor ritonavir, proton pump inhibitor pantoprazole, as well as the dietary constituent curcumin, are known inhibitors of this transporter (Mao and Unadkat, 2015).

BCRP is recognized by the Food and Drug Administration (FDA) and International Transporter Consortium (ITC) as an important transporter that is prone to potential clinical drug-drug interactions (DDI) (Giacomini et al., 2010; Tweedie et al., 2013; USFDA-CDER, 2017a; USFDA-CDER, 2017b) because of its recognition of a wide range of substrates and inhibitors. Except for biopharmaceutical classification system class I (BCS class I, high solubility and high permeability) compounds, BCRP substrates (victims) are prone to BCRP inhibitor (perpetrator)-mediated DDI when they are dosed concomitantly, through the oral route (Lee et al., 2015; USFDA-CDER, 2017b).

ITC and FDA have detailed the decision tree and guidelines for determining BCRP substrates, inhibitors, and the possibility of clinical DDIs (Giacomini et al., 2010; USFDA-

Downloaded from dmd.aspetjournals.org at ASPET Journals on April 23, 2024

DMD Fast Forward. Published on August 15, 2018 as DOI: 10.1124/dmd.118.083584
This article has not been copyedited and formatted. The final version may differ from this version.

CDER, 2017b). *In vivo* assessment of BCRP substrates have utilized transporter knockout models or imaging techniques such as positron emission tomography and gamma-scintigraphy which are known to have their own limitations (Giacomini et al., 2010). While rosuvastatin and sulfasalazine have been proposed as BCRP pre-clinical and clinical *in vivo* probe substrates, they are not specific BCRP substrates (Dahan and Amidon, 2010; Ellis et al., 2013). Hence, multiple factors can complicate interpretation of results with these probe substrates. For sulfasalazine, differences in its metabolism by colonic bacteria to sulfapyridine, or genetic variation in or inhibition of N-acetyltransferase 2 which metabolizes sulfapyridine, or its transport by OATP2B1; or for rosuvastatin, inhibition of transporters such as OATP1B1, can lead to variability in probe disposition independent of Bcrp inhibition (Lee et al., 2015). Moreover, quantitative analysis of sulfasalazine and rosuvastatin in human tissues requires expensive and sophisticated analytical instrumentation.

An ideal assay for Bcrp activity would use a specific, inexpensive, fluorescent near infrared (NIR) substrate probe that could be monitored in real time both *in vitro* (high-throughput) and *in vivo*. Pheophorbide A (PhA) is a breakdown product of chlorophyll and is a specific dietary substrate of Bcrp (Jonker et al., 2002; Robey et al., 2004; Kraatz et al., 2014), with an efflux ratio of 3.15 in cell lines overexpressing Bcrp (Zhang et al., 2009). Two labs have developed *in vitro* assays for BCRP function/inhibition using PhA, also showing that PhA is not a substrate for P-glycoprotein or MRP1 *in vitro* (Robey et al., 2004; Robey et al., 2005). PhA is a low solubility, low permeability compound with no reported metabolic instabilities. We examined whether PhA is a BCRP probe substrate that can be used both *in vitro* and *in vivo* to investigate BCRP function according to the FDA and ITC guidelines (Giacomini et al., 2010) (USFDA-CDER, 2017b). We hypothesized that PhA can be utilized as an *in vivo* probe to assess

Downloaded from dmd.aspetjournals.org at ASPET Journals on April 23, 2024

DMD Fast Forward. Published on August 15, 2018 as DOI: 10.1124/dmd.118.083584
This article has not been copyedited and formatted. The final version may differ from this version.

DDI associated with the inhibition of Bcrp at the gastrointestinal tract in mice. We utilized a live animal fluorescence imaging technique, using PhA, to screen in real-time for orally administrated BCRP inhibitors and predict intestinal BCRP-mediated DDIs. Our results demonstrate that *in vivo* fluorescence imaging of PhA can be used to identify BCRP inhibitors in order to assess pre-clinically the potential for BCRP-mediated clinical DDIs.

Downloaded from dmd.aspetjournals.org at ASPET Journals on April 23, 2024

DMD Fast Forward. Published on August 15, 2018 as DOI: 10.1124/dmd.118.083584
This article has not been copyedited and formatted. The final version may differ from this version.

MATERIALS AND METHODS

Chemicals and reagents. The following chemicals and reagents were purchased: Pheophorbide A (Frontier Scientific, Newark, DE, USA), lapatinib and curcumin (Cayman Chemicals, Ann Arbor, MI, USA), elacridar (Astatech Inc., Bristol, PA, USA), pantoprazole (Santa Cruz Biotech, Dallas, TX, USA), sorafenib and dasatinib (Chemietek, Indianapolis, IN, USA), chlorophyll A and protoporphyrin IX (Sigma-Aldrich, St. Louis, MO).

Animals. Wild type (WT) and Bcrp KO Friend Virus B (FVB) male mice (n = 4 each group, 10 weeks old) were purchased from Taconic Biosciences, Inc. (Hudson, NY) for the knockout mice study. For all other Bcrp inhibitor studies, control mice of FVB background (n = 4 for control and each inhibitor treatment group) were purchased from The Jackson Laboratory (Bar Harbor, ME, USA). All mice were fed either a regular alfalfa containing diet (Purina catalog# 5013, Largo, FL) or an alfalfa-free (AFF) diet (Purina, catalog# AIN-93G, Largo, FL) for at least three days, the time necessary to reduce background PhA auto-fluorescence (Inoue et al., 2008), and they were provided water *ad libitum*. The Institutional Animal Care and Use Committee of St. Jude Children's Research Hospital, in accordance with the U.S. National Institutes of Health guidelines, approved all experimental procedures.

Cell lines. Madine-Darby Canine Kidney (MDCKII) cells overexpressing human full-length wild type BCRP and the parenteral cell lines were kindly provided by Dr. Alfred Schinkel (The Netherlands Cancer Institute, Amsterdam, Netherlands) and were cultured as described (Pavek et al., 2005).

Determination of Pheophorbide a concentration in rodent food pellets. Six food pellets each from regular diet and AFF diet were weighed and soaked with half parts of water. After 30 minutes, one gram of food pellet was mixed with 5 mL methanol and stirred overnight

Downloaded from dmd.aspetjournals.org at ASPET Journals on April 23, 2024

DMD Fast Forward. Published on August 15, 2018 as DOI: 10.1124/dmd.118.083584
This article has not been copyedited and formatted. The final version may differ from this version.

for PhA extraction. The following day, samples were centrifuged at 15000 g for 15 minutes and the supernatant collected. The supernatant was further centrifuged, filtered and used for measurement of PhA using a modified HPLC-Fluorescence Detector (HPLC-RF)-based method published previously (Almela et al., 2000). 40 µL of the final supernatant was injected onto the HPLC system (Shimadzu Prominence, Kyoto, Japan) consisting of a LC-20AB quaternary high-pressure gradient pump, SIL-20AC$_{HT}$ auto sampler and RF-10 A$_{XL}$ fluorescence-detector. Chromatographic separation of PhA was achieved using Hypersil ODS C18 column (150X4 mm; 5 µm particle size) fitted with Hypersil ODS (C18) Javelin Guard Column (10X4 mm; 5 µm particle size) and a gradient elution method with a run time of 10 minutes. The mobile phase for elution was 80% methanol in 0.5M ammonium acetate (Phase A) and 100% methanol (Phase B) with a gradient of: 0 to 2 minutes 60 to 95% methanol, 2 to 8 minutes 95% methanol, 8 to 9 minutes 95 to 60% methanol, and the run stopped at 10 minutes. Retention time for PhA was 3.5 minutes. The PhA peak was identified and fluorescence was measured at 400 (Ex) and 670 (Em) nm (Supplemental Fig S1). Analyte area was used for calibration and measurement of unknown concentrations against a known PhA concentration prepared in mobile phase A. The calibration range was 0.02 µM to 10 µM.

Treatments. Mice were kept on an AFF diet for at least three days to eliminate PhA the background autofluorescence**.** WT and Bcrp KO mice (10 weeks, n = 4/group) were administrated PhA (10 mg/kg) by oral gavage at a dose volume of 10 ml/kg body weight, and imaging or blood collection was performed at appropriate time points up to 6 hrs. after dosing. For the inhibitor study, oral doses of the inhibitors were selected based on clinical relevance or previously demonstrated effects (Table 1) and formulated for oral dosing by suspending an appropriate amount of the compound in 0.5% hydroxypropyl-methyl- cellulose (HPMC) and 1%

Downloaded from dmd.aspetjournals.org at ASPET Journals on April 23, 2024

DMD Fast Forward. Published on August 15, 2018 as DOI: 10.1124/dmd.118.083584
This article has not been copyedited and formatted. The final version may differ from this version.

Tween 80 (Sigma, St. Louis, MO) in water by trituration method. Bcrp inhibitors elacridar (ECD) (100 mg/kg), lapatinib (LPB) (90 mg/kg), dasatinib (DSB) (10 mg/kg), sorafenib (SFB) (40 mg/kg), curcumin (CCM) (300 mg/kg) and pantoprazole (PPZ) (40 mg/kg) were administrated orally, one hour prior to oral dosing of PhA. Imaging and blood collection was performed at appropriate times up to 6 hours after PhA dosing. All animals were fasted up to 6 hours after PhA dosing.

***In vivo* fluorescence imaging.** Mice were anesthetized by isoflurane anesthesia (2%, inhalation) and placed ventrally in the chamber of a Xenogen in vitro imaging system (IVIS) 200 (PerkinElmer, USA) imaging system. Fluorescence images were obtained under anesthesia with a fixed exposure time of one second and NIR filter setting of 675 nm excitation and 840 nm emission. Mice were repetitively imaged at 0 hr (baseline), and 1, 2, 3, 4 and 6 hours after PhA administration. Images were scaled to a maximum intensity of 1×10^8 photons/s/cm^2/sr for visualization. All images were analyzed with Living Image® v4.5 (PerkinElmer, USA) to obtain the fluorescence intensity in the selected region of interest (ROI) of fluorescence (flux/sec), which was selected as a fixed rectangular area around each mouse. For the control and inhibitor treatment groups, ROI (flux/sec) for each mouse was normalized by its flux measured at 0 hr. For the WT and Bcrp KO mice, ROI of the WT mice at 0 hour was used for normalizing all fluorescence (ROI) data. Normalized ROI data was used for calculation of $AUC_{FL\ 0\text{-}6hr}$ in GraphPad Prism v 5.02.

Pharmacokinetic study of PhA. Immediately after the imaging, 50 µL of blood was collected by saphenous vein into a microvette capillary blood collection tube (Sarstedt, obtained from Fisher Scientific, Pittsburgh, PA) and serum was separated by centrifuging the sample at

Downloaded from dmd.aspetjournals.org at ASPET Journals on April 23, 2024

DMD Fast Forward. Published on August 15, 2018 as DOI: 10.1124/dmd.118.083584
This article has not been copyedited and formatted. The final version may differ from this version.

5000 rpm for 10 min. Blood samples were collected at 0, 1, 2, 4 and 6 hrs. for measurement of PhA concentration in the serum.

Measurement of PhA concentration in whole serum. A fluorescence-based method was used to measure PhA concentration in whole serum. A calibration of known PhA concentrations was prepared by spiking known PhA concentrations prepared in DMSO into 24 µL of blank serum, collected from mice on the AFF diet. 25 µL of standard serum concentrations and serum samples collected for the study were diluted to 100 µL with distilled water in a 96 well clear bottom black polystyrene plate (Cat# 3603, Corning, NY, USA). PhA fluorescence was measured at 400 nm (Ex) and 670 nm (Em) on a Synergy H4 Hybrid Reader (BioTek, Winooski, VT, USA). All fluorescence values were blank-corrected and unknown sample PhA concentrations were interpolated from a freshly prepared PhA standard curve (0.02 µM to 10 µM) and the PhA concentration for each mouse was used to measure $AUC_{Serum\ 0\text{-}6hr}$ in GraphPad Prism v 5.02. A fluorescence emission spectral scan from 500 to 700 nm was performed for all samples with fixed excitation at 400 nm and compared with the corresponding standard PhA concentration prepared in blank serum, with and without PhA, to confirm the identity of PhA in study samples at the emission wavelength of 670 nm (Supplemental Fig S2).

***Ex vivo* fluorescence imaging of mouse intestine**. After *in vivo* imaging, mice were immediately euthanized and blood was collected by cardiac puncture. The small intestine was dissected out and fluorescence (675 nm excitation and 840 nm emission) images were obtained before and after flushing out the intestinal contents with phosphate buffered saline (PBS) (5 ml, three times). Fluorescence images were obtained using one second exposure with a filter setting for near infrared. Images were scaled to a maximum intensity of 1×10^8 photons/s/cm2/sr.

Downloaded from dmd.aspetjournals.org at ASPET Journals on April 23, 2024

DMD Fast Forward. Published on August 15, 2018 as DOI: 10.1124/dmd.118.083584
This article has not been copyedited and formatted. The final version may differ from this version.

Fluorescence microscopy of intestinal sections. Intestinal segments of WT and Bcrp KO mice on a regular diet were washed with cold PBS, filled with warm 3% low melting agarose in 0.9% (w/v) NaCl, immediately soaked in ice cold Dulbecco's Modified Eagle's Medium to solidify the agarose, paraffin embedded, and precision transverse slices cut onto slides. Fluoroshield mounting medium with DAPI (4', 6-diamidino-2-phenylindole dihydrochloride) was applied to the tissue, spread evenly, and cover slips applied for fluorescence microscope imaging (Nikon ECLIPSE T_i).

***In vitro* assay for measuring IC_{50} of Bcrp inhibitors.** A 96 well plate-based assay utilizing control and BCRP overexpressing Madine-Derby Canine Kidney (MDCKII) cells(Weiss et al., 2007) was used for measuring the IC_{50} of selected BCRP inhibitor drugs using PhA as a probe BCRP substrate (Robey et al., 2004). Briefly, 1*10^4 cells/ well were plated in a 96 well plate and incubated at 37°C until the cells were at least 80 - 90% confluent. On the day of the experiment, media was removed, cells were washed with PBS and incubated for 30 min with or without BCRP inhibitors prepared in 100 µL of modified Krebs Ringer buffer (115 mM NaCl, 5.9 mM KCl, 1.2 mM $MgCl_2$, 1.2 mM NaH_2PO_4, 2.5 mM $CaCl_2$, 2.5 mM $NaHCO_3$ and 10 mM Glucose) (Mahringer et al., 2009). After pre-incubation with inhibitors, media was removed and cells were incubated with 1 µM PhA with or without the inhibitor prepared in 100 µL Krebs-Ringer buffer for 2 hrs. Fumitremorgin C (FTC) at a concentration of 5 µM was used as a standard BCRP inhibitor. After 2 hrs, cells were washed with chilled Dulbecco's phosphate buffer saline (DPBS) twice, 100 µL DPBS added, and fluorescence measured on Synergy H4 Hybrid Reader at 400 nm (Ex) and 670 nm (Em). Immediately after fluorescence measurement, 100 µL Promega CellTiter-Glo® reagent (Fisher Scientific, Lenexa, KS, USA), was added to each well, incubated at 37°C for 5 minutes, and luminescence measured. To calculate the cell

Downloaded from dmd.aspetjournals.org at ASPET Journals on April 23, 2024

DMD Fast Forward. Published on August 15, 2018 as DOI: 10.1124/dmd.118.083584
This article has not been copyedited and formatted. The final version may differ from this version.

number/well 120,000 MDCKII control and BCRP overexpressing cells were plated per well and diluted with cell culture media 1:1 up to 937 cells/well (n=6 each dilution each cell type), incubated at 37^{o}C for 6 hours for the cells to attach. After 6 hrs, cells are washed with chilled DPBS, after which 100 µL DPBS and CellTiter-Glo ® reagent at room temperature was added to the cells, incubated for 5 min at 37^{o}C and luminescence measured. First, the results were background-corrected, normalized with cell number in each well to calculate PhA fluorescence/ 10^3 cells/ well. Fold change of PhA accumulation in MDCKII cells in the presence of BCRP was calculated by dividing MDCKII-BCRP fluorescence/cell with that of MDCKII. The % inhibition by BCRP inhibitors was calculated by the following equation:

$$\% \text{ Inhibition} = \frac{(\text{Fluorescence Inhibitor} - \text{Fluorescence no inhibitor})}{(\text{Fluorescence FTC} - \text{Fluorescence no inhibitor})} * 100$$

IC_{50} values of the inhibitors were calculated using GraphPad prism v5.02. All assays were run at least three times with n = 6 wells for each concentration of inhibitor, or standard inhibitor, in each assay. Results of all experiments were combined (n=18) to calculate final parameters.

Statistical Analysis. All serum PhA concentration–time data were plotted as mean PhA concentration ± SEM and similarly, the whole-body fluorescence data over zero-hour of each individual mouse (for the inhibitor study), or over WT mice zero-hour fluorescence (for Bcrp KO study), were plotted as mean ratio ± SEM. GraphPad Prism v5.02 was used to calculate the area under the concentration – time or fluorescence (flux/sec) ratio – time curve for individual mice up to 6 hours ($AUC_{Serum\ 0\text{-}6h}$ or $AUC_{FL\ 0\text{-}6h}$). Mean AUC±SEM are plotted and compared with the control or WT using the unpaired t-test, significance is calculated at $p<0.05$. All calculations were done on GraphPad Prism v5.02.

Downloaded from dmd.aspetjournals.org at ASPET Journals on April 23, 2024

DMD Fast Forward. Published on August 15, 2018 as DOI: 10.1124/dmd.118.083584
This article has not been copyedited and formatted. The final version may differ from this version.

RESULTS

Bcrp KO mice on a regular alfalfa containing diet have higher whole-body fluorescence, arising from PhA and chlorophyll, than WT mice. Wild-type (WT) mice, fed a regular alfalfa containing diet and imaged with an In Vivo Imaging System (IVIS) across the NIR fluorescence spectrum, had detectable autofluorescence emission signals with a 675 nm excitation and 840 nm emission setting, that was localized to the intestinal region (Fig 1A). Bcrp KO mice fed the same alfalfa containing diet had a higher whole-body autofluorescence (Fig 1A). Alfalfa is known to be a source of chlorophyll, and its catabolite pheophorbide A (PhA), a known specific BCRP substrate, both of which emit in the NIR. Feeding both WT and Bcrp-KO mice an alfalfa free diet (AFF) for three days eliminated the autofluorescence (Fig 1A), as reported by others (Leblond et al., 2010). To further confirm that the diet was the source of the observed fluorescence, we IVIS imaged the alfalfa +/- food pellets, using the same imaging parameters, and observed fluorescence only from the regular alfalfa food pellets (Fig 1B). We compared the fluorescent signal intensity of chlorophyll a (CLPa), PhA, and protoporphyrin IX (PPIX), a fluorescent Bcrp endogenous substrate, over a concentration range of 0.31 to 10 μM, using the same imaging parameters (Fig 1C). Only PhA was detectable at the lowest concentration tested (0.31 μM), almost 10-fold lower than the lowest detectable concentration of CLPa (2.5 μM), and PhA had a higher fluorescent intensity compared to chlorophyll at each concentration (Fig 1C). PPIX fluorescence was undetectable under these imaging parameters. Hence, both chlorophyll and PhA could be the source of autofluoresence in the alfalfa containing diet.

Pheophorbide A is present in regular mouse diet, but not in AFF diet. To further confirm the presence of PhA in the alfalfa containing regular diet, we analyzed the amount of PhA in mouse food pellets, following methanol extraction, using an HPLC-RF- based method. PhA, and

Downloaded from dmd.aspetjournals.org at ASPET Journals on April 23, 2024

DMD Fast Forward. Published on August 15, 2018 as DOI: 10.1124/dmd.118.083584
This article has not been copyedited and formatted. The final version may differ from this version.

another abundant fluorescent compound, was present in the regular alfalfa containing food pellet (Supplemental Fig S1B), but not in the alfalfa free food pellet extract (Supplemental Fig S1C). We determined the PhA concentration in the alfalfa containing regular diet to be 1.71 µg/gm of food pellet. Assuming daily food intake for a 30 gm mouse is 6 gms, it can be estimated that a mouse on a regular alfalfa containing diet consumes ~343 µg PhA/kg body weight daily.

Bcrp gene deletion leads to higher absorption/retention of PhA in mouse enterocytes.

During *in vivo* live animal imaging, we observed the maximum fluorescence in the intestinal region of Bcrp WT and KO mice (Fig 1A), which was expected since PhA is a dietary constituent. However, unexpectedly, the fluorescence intensity was greater in the Bcrp KO mouse intestine. This result was unanticipated since we would have assumed greater absorbance of PhA from the food in the KO mouse, and hence, a lower PhA intestinal signal intensity compared to WT mice. To determine if the higher PhA intestinal fluorescence was due to PhA trapping in the intestinal enterocytes of KO mice, we compared the localization and intensity of fluorescence in WT and Bcrp KO mice fed a regular alfalfa containing diet, by *ex vivo* imaging of isolated intestines. High fluorescence intensity was observed in the small intestine of both WT and Bcrp KO mice before flushing the intestinal contents (not shown), but after flushing, the small intestine of Bcrp KO mice, but not WT mice, retained a high level of fluorescence (Fig 2). The intestinal segments were then filled with warm agarose, paraffin embedded, and transverse sections cut and imaged by fluorescence microscopy. The enterocytes of BCRP KO mice showed a much higher level of fluorescence compared to those of the WT mice (Fig 2) suggesting that the absence of Bcrp at the enterocytes was leading to higher enterocyte PhA absorption and trapping in the Bcrp KO mice fed a regular alfalfa containing diet.

Downloaded from dmd.aspetjournals.org at ASPET Journals on April 23, 2024

DMD Fast Forward. Published on August 15, 2018 as DOI: 10.1124/dmd.118.083584
This article has not been copyedited and formatted. The final version may differ from this version.

Oral absorption of PhA is greater in Bcrp KO versus WT mice. Since both dietary chlorophyll and PhA from alfalfa containing foods would fluoresce in the NIR, and because we could not control either the amount of these constituents in the diet, or the amount of chlorophyll that might be converted to PhA, or the amount each mouse consumed, we maintained the mice on an AFF diet for at least three days and administered PhA by oral gavage to determine if PhA could be a probe substrate for monitoring Bcrp function *in vivo*. Following PhA (10 mg/kg) oral gavage, and then fasting, PhA disposition was IVIS monitored longitudinally over the next 6 hrs. Representative images at two hrs post-PhA dosing displayed significantly greater whole-body fluorescence in the Bcrp KO compared to WT mice (Fig 3A). The whole-body fluorescence at different time-points, normalized to the fluorescence in WT mice at baseline, when plotted against time after dosing, exhibited significantly higher fluorescence in Bcrp KO mice across all observed time points (1, 2, 4 and 6 hrs) (Fig 3B). Quantification of the area under the fluorescence ratio time curve up to 6 hrs ($AUC_{FL\ 0\text{-}6h}$) showed a significant increase (3.5-fold) of fluorescence in the Bcrp KO compared to WT mice (Fig 3C). We also measured the serum concentration of PhA in the same experiment at 1, 2, 4 and 6 hrs. The serum concentration of PhA in the Bcrp KO mice was also found to be significantly higher across all observed time points compared to WT mice (Fig 3D) with a 50-fold increase in area under concentration-time curve calculated up to 6 hrs ($AUC_{Serum\ 0\text{-}6h}$) (Fig 3E). These results, showing a significantly higher fold increase of both whole-body and serum PhA fluorescence over baseline, in Bcrp KO mice compared to WT, suggest that orally administered PhA can be utilized to capture a range of inhibition potency by Bcrp inhibitors, and thereby identify Bcrp-mediated drug-drug interactions (DDIs) in mice.

Downloaded from dmd.aspetjournals.org at ASPET Journals on April 23, 2024

DMD Fast Forward. Published on August 15, 2018 as DOI: 10.1124/dmd.118.083584
This article has not been copyedited and formatted. The final version may differ from this version.

Selected Bcrp inhibitors exhibited comparable *in vitro* IC50 values with PhA as reported previously. To further test our hypothesis that PhA can be used as an *in vivo* probe (victim) for identification of intestinal Bcrp-mediated DDIs, we selected known Bcrp inhibitors (perpetrators) as per FDA guidance based on their $[I_2]/IC_{50} = I_{gut}/ IC_{50}$ (Clinical dose/250 ml)/ IC_{50}) where I_{gut} is the maximum human dose in the apparent human gut fluid volume of 250 ml (Table1). While IC_{50} values of the selected inhibitors (except dasatinib) were reported in the literature, a wide variety of Bcrp probe substrates as well as cell lines were used for these IC_{50} measurements. Using PhA as a BCRP probe substrate, we used MDCKII-BCRP cell-based assays to determine the IC_{50} of the selected BCRP inhibitors (Fig 4). Lapatinib was found to be the strongest BCRP inhibitor with a measured IC_{50} of 40 nM, followed by elacridar (0.21 μM), sorafenib (2.18 μM), curcumin (2.58 μM), pantoprazole (11.19 μM), and dasatinib (22.76 μM). The IC_{50} of these inhibitors for Bcrp-mediated PhA transport, were found to be similar to those reported in the literature using different BCRP probe substrates (Table 1), except for PPZ, for which the observed IC_{50} for PhA was 2-fold higher than the reported IC_{50} (5.5 μM). Assuming a 0.8 mL mouse stomach volume, C_{gut}/ IC_{50} was ≥ 10 for all the inhibitors (Table 1), indicating a possible drug-drug interaction potential with orally dosed BCRP substrates in mice, where, C_{gut} is the selected inhibitor dose/0.8 mL.

Bcrp inhibitors increase whole body and serum fluorescence of PhA. Based on reported literature, the selected drugs were expected to cause drug-drug interactions with Bcrp substrates when administered concomitantly, via an oral route, and increase systemic exposure (blood/ plasma / serum AUC) of the substrate. Therefore, we dosed the inhibitors orally, using

Downloaded from dmd.aspetjournals.org at ASPET Journals on April 23, 2024

DMD Fast Forward. Published on August 15, 2018 as DOI: 10.1124/dmd.118.083584
This article has not been copyedited and formatted. The final version may differ from this version.

concentrations in mice equivalent to those recommended to screen for human BCRP DDIs *in vivo* (Lee et al., 2015) along with the Bcrp probe substrate PhA, and measured whole body fluorescence and serum PhA concentrations (Fig 5A). Whole-body fluorescence imaging of mice treated with the Bcrp inhibitors lapatinib, elacridar and curcumin displayed higher fluorescence compared to the control-treated mice. After quantification of fluorescence flux/second and normalization with baseline fluorescence from the same mice, these values were plotted against time after dosing (Fig 5B and 5C), and $AUC_{FL\ 0\text{-}6h}$ was calculated for all the inhibitor-treated and control mice. Lapatinib exhibited the maximum fold increase (2.4-fold) of $AUC_{FL\ 0\text{-}6h}$ over control mice, followed by curcumin (2.3-fold), elacridar (2.2-fold), pantoprazole (1.5-fold) and sorafenib (1.44-fold) (Fig 5D). Dasatinib did not significantly increase the $AUC_{FL\ 0\text{-}6h}$ over control mice.

The PhA serum concentration-time plots after treatment with Bcrp inhibitors displayed a similar trend as observed with whole body fluorescence (Fig 5E and 5F), with a similar rank order of inhibitor-mediated increase in $AUC_{Serum\ 0\text{-}6h}$ observed as was seen for $AUC_{FL\ 0\text{-}6h}$ (Fig 5G). Lapatinib treatment caused the largest increase in PhA serum fluorescence (13.8-fold), followed by curcumin (7.79-fold), elacridar (5.2-fold), pantoprazole (2.02-fold) and sorafenib (1.45-fold). No significant effect of dasatinib was found on serum PhA concentration consistent with the lack of effect on PhA whole-body fluorescence. Whereas $C_{gut}/\ IC_{50}$ for all inhibitors were ≥ 10, $C_{gut\_soluble}/\ IC_{50}$ values (Table 1) displayed a better correlation with the observed fold change by Bcrp inhibitors, where $C_{gut\_soluble}$ is the predicted solubility of the inhibitors obtained from DrugBank database (https://www.drugbank.ca). Although PhA, and related porphyrins, are not substrates of P-glycoprotein or multidrug resistance protein 1 *in vitro* (Robey et al., 2004)(Bakhsheshian et al., 2013), since many of the inhibitors tested can also affect Pgp-

Downloaded from dmd.aspetjournals.org at ASPET Journals on April 23, 2024

DMD Fast Forward. Published on August 15, 2018 as DOI: 10.1124/dmd.118.083584
This article has not been copyedited and formatted. The final version may differ from this version.

mediated transport, we compared the effect of elacridar on PhA disposition in Bcrp WT and KO mice. A very small effect of elacridar was seen on PhA serum fluorescence in the Bcrp KO mice but there was no significant effect of elacridar on PhA whole body fluorescence in Bcrp KO mice (Supplemental Fig S3).

Downloaded from dmd.aspetjournals.org at ASPET Journals on April 23, 2024

DMD Fast Forward. Published on August 15, 2018 as DOI: 10.1124/dmd.118.083584
This article has not been copyedited and formatted. The final version may differ from this version.

DISCUSSION

These studies demonstrate that the DDI potential of intestinal Bcrp inhibitors can be characterized pre-clinically *in vivo* using the Bcrp probe substrate PhA. PhA whole body fluorescence imaging over time, coupled with serum sampling for PhA systemic quantification, allows for longitudinal, real-time kinetic analysis of the effect of Bcrp inhibitors directly on changes in tissue exposure. Murine Bcrp limited PhA intestinal oral absorption as evidenced by the significant difference in PhA AUC between Bcrp KO and WT mice (50-fold higher PhA serum concentration in KO mice). Indeed, the enterocytes themselves, following wash-out of intestinal food contents, showed a significantly higher concentration of PhA that was retained in the absence of the Bcrp efflux transporter (Fig 2). The dynamic range of PhA fluorescence, both whole body and in serum, between WT and Bcrp KO mice, allowed us to rapidly examine the effect of Bcrp inhibitors on the whole body and serum PhA fluorescence. We specifically chose drugs that, when administered at clinically relevant doses to mice, would be predicted to cause a Bcrp-mediated DDI in vivo. For an orally administered Bcrp inhibitor drug, if the calculated [(dose/250 ml) / IC_{50} for Bcrp] is ≥ 10, (i.e., $I_{gut}/ IC_{50} \geq 10$), FDA recommends analysis for a possible oral Bcrp inhibition-mediated DDI (USFDA-CDER, 2017b). Indeed, for pantoprazole, elacridar, curcumin, and lapatinib the predicted clinical DDI liability, I_{gut}/ IC_{50}, obtained from literature reports, are significantly higher than 10 (Lee et al., 2015).

Taken together, the serum concentration and imaging data provide complimentary evidence that PhA can be used for identification of oral DDIs associated with Bcrp. Indeed the rank order of efficacy for the series of Bcrp inhibitors increasing the PhA serum concentration over time (lapatinib (13.8-fold) > curcumin (7.8 fold) > elacridar (5.17 fold)

Downloaded from dmd.aspetjournals.org at ASPET Journals on April 23, 2024

DMD Fast Forward. Published on August 15, 2018 as DOI: 10.1124/dmd.118.083584
This article has not been copyedited and formatted. The final version may differ from this version.

>pantoprazole (2.02 fold) > sorafenib (1.45 fold), precisely matched the rank order for the same BCRP inhibitors increasing PhA's $AUC_{FL\ 0\text{-}6h}$ whole-body fluorescence in the same mice. Indeed, for this series of perpetrators, the Bcrp inhibitor log transformed gut concentration/IC_{50} vs. fold change in either AUC of PhA body fluorescence or AUC of PhA serum fluorescence gives a linear relationship (Supplemental Fig S4), further validating that this assay is measuring the oral Bcrp DDI. Moreover, the rank order of intestinal perpetrator Bcrp inhibition potential (when victim drugs, such as sulfasalazine, have been tested) was similar to the experimentally determined rank order of PhA-inhibitor efficacy. Hence, the hierarchy of intestinal Bcrp inhibition was similar when the perpetrators were the same, but the victim was either sulfasalazine or PhA. For example, when mice were orally administered curcumin (300 mg/kg) with PhA, we observed a 7.79-fold increase in serum fluorescence of PhA, while others observed an 8-fold increase in sulfasalazine plasma exposure in presence of curcumin (300 to 400 mg/kg) (Kusuhara et al., 2012), further supporting our proposal that PhA is useful as an *in vivo* probe for Bcrp function. Notably, FDA Drug Interactions & Labeling guidelines indicate that a ≥ 1.5-fold increase in sulfasalazine AUC (with concomitant dosing with a Bcrp inhibitor) is considered as evidence for *in vivo* inhibition of Bcrp. According to this criteria, our studies indicate that pantoprazole, elacridar, curcumin and lapatinib produced a PhA AUC ≥ 1.5-fold *in vivo*, thus indicating inhibition of Bcrp.

Our experimental findings indicate that PhA that could be useful for pre-clinical evaluation of clinical Bcrp-mediated DDI using WT mice in the presence of Bcrp inhibitors. Mouse Abcg2/Bcrp has 81% sequence homology with human ABCG2/BCRP (Allen et al., 1999), and there is significant functional overlap in substrate and inhibitor specificity (Bakhsheshian et al.,

Downloaded from dmd.aspetjournals.org at ASPET Journals on April 23, 2024

DMD Fast Forward. Published on August 15, 2018 as DOI: 10.1124/dmd.118.083584
This article has not been copyedited and formatted. The final version may differ from this version.

2013). Multiple lines of evidence demonstrate that PhA is transported by Bcrp, but not by other ABC transporters. First, PhA was identified as a unique Bcrp substrate in an initial Bcrp KO mouse report (Jonker et al., 2002), and this has been confirmed and extended to mouse Bcrp and human BCRP cell lines (Bakhsheshian et al., 2013) (Robey et al., 2004). Indeed, Bakhsheshian (2013) demonstrated that a series of porphyrins, including PhA, behaved similarly with both mouse Bcrp and human BCRP displaying similar substrate and inhibitor specificity. Second, elacridar did not cause a significant increase in PhA whole body NIR fluorescence or serum concentration in Bcrp KO mice. Third, among all of the ABC transporter KO mice, and numerous publications with each of them, only absence of Bcrp resulted in an accumulation of PhA (a breakdown product of alfalfa in all standard rodent chow) and phototoxicity (Jonker et al., 2002).

The PhA excitation and emission wavelengths in mice *in vivo* (670 nm (Ex) and 840 nm (Em)) **differed from *in vitro*** (400-410 nm (Ex) and 670 nm (Em)). This is not unexpected because live animal fluorescence at any wavelength is routinely affected by absorbance and light scattering due to the complex environment comprised of plasma proteins and tissue barriers (Leblond et al., 2010). Thus, it is important to consider this *a priori* when selecting Ex/Em wavelength settings to use *in vivo*. Of note, if we had used the *in vitro* Ex/Em PhA wavelength parameters, we would have missed the *in vivo* PhA fluorescence signal.

PhA has low solubility and permeability, and as a Bcrp substrate, is poorly absorbed which was reflected in PhA being detected in the intestine of PhA gavaged mice, but undetectable in the serum of WT mice gavaged with PhA. PhA has been reported to be mainly cleared unabsorbed

Downloaded from dmd.aspetjournals.org at ASPET Journals on April 23, 2024

DMD Fast Forward. Published on August 15, 2018 as DOI: 10.1124/dmd.118.083584
This article has not been copyedited and formatted. The final version may differ from this version.

in feces(Kraatz et al., 2014). Interestingly, we routinely found that *ex vivo* fluorescence comparison of the intestinal segments of WT mice fed a normal PhA-containing diet, after flushing out the intestinal contents, revealed a lower PhA fluorescence in the duodenum compared to a higher PhA fluorescence in the jejunum and ileum. The gradient of Bcrp expression in the mouse intestine (i.e., higher in the duodenum and lowest in the ileum) (Gutmann et al., 2005) appears to be inverse to the PhA fluorescence in the eterocytes of WT mice (i.e., lowest in the duodenum and higher in the jejunum and ileum). The increased fluorescence in the intestinal region in Bcrp KO mice (Fig 2A), in spite of increased systemic absorption from the lumen, was due to trapping of PhA in the enterocytes in the absence of Bcrp mediated efflux (Fig 2B), and this was captured in the *in vivo* imaging.

Serum PhA fluorescence following oral co-administration of PhA and inhibitors might be a more useful tool than whole body fluorescence for elucidating the DDI of weak Bcrp inhibitors. We found a significantly higher (3.5-fold) area under the fluroescence ratio – time curve for whole body fluorescence up to 6 hrs ($AUC_{FL\ 0\text{-}6h}$) (Fig 3B and 3C) in BCRP KO compared to WT mice. However, in these same animals, the PhA serum area under the concentration – time curve up to 6 hours ($AUC_{Serum\ 0\text{-}6h}$) (Figs 3D and 3E) was increased over 50-fold. The discrepancy in the increase in PhA serum concentration (50-fold) vs. whole body fluorescence (3.5 fold) is likely due to a higher background fluorescence from the unabsorbed dietary PhA in the intestine. **Nevertheless, there are unique advantages to using whole body fluorescence of the Bcrp substrate PhA to screen for oral DDI including:** (a) the ease and noninvasive nature of its detection, (b) that animals do not need to be sacrificed and can be used repeatedly, (c) the ability to longintudinally monitor changes in Bcrp substrate tissue distribution

Downloaded from dmd.aspetjournals.org at ASPET Journals on April 23, 2024

DMD Fast Forward. Published on August 15, 2018 as DOI: 10.1124/dmd.118.083584
This article has not been copyedited and formatted. The final version may differ from this version.

into other organs (*ex vivo*) in the presence of systemic inhibition of Bcrp (the subject of another manuscript).

To our knowledge, this is the first report that shows the fluroescent Bcrp substrate PhA can be utilized for identification of *in vivo* DDI due to inhibition of Bcrp at the gastrointestinal tract and creates an opportunity for a high throughput *in vivo* Bcrp inhibitor assay. Also, utilization of serum fluorescence by simple spectrometry makes this method unique in that minimal technical resources are required for identification of Bcrp substrates. Furthermore, this method is in conformation with the 3R principal (replacement, reduction and refinement), as it would reduce the requirement of invasive studies thus significantly reducing the number of lab animals, at the same time creating high quality reliable data. In conclusion, our study shows that dynamic fluorescence imaging in live animals utilizing PhA as a Bcrp probe can be used for identification of Bcrp inhibitors and to understand the DDI liability of such inhibitors. Further studies are required to determine if we can use PhA as a probe substrate of BCRP activity in the clinic, and if it may be further utilized to understand systemic Bcrp inhibition.

Downloaded from dmd.aspetjournals.org at ASPET Journals on April 23, 2024

DMD Fast Forward. Published on August 15, 2018 as DOI: 10.1124/dmd.118.083584
This article has not been copyedited and formatted. The final version may differ from this version.

ACKNOWLEDGEMENTS

The authors would like to thank the St Jude Center for In Vivo Imaging and Therapeutics Core, (Dr. Walter Akers and Cheryl Winter).

Downloaded from dmd.aspetjournals.org at ASPET Journals on April 23, 2024

DMD Fast Forward. Published on August 15, 2018 as DOI: 10.1124/dmd.118.083584
This article has not been copyedited and formatted. The final version may differ from this version.

AUTHORSHIP CONTRIBUTIONS

Participated in research design: Ganguly, Yasuda, Schuetz

Conducted experiments: Yasuda, Ganguly

Contributed new reagents or analytical tools: NA

Performed data analysis: Ganguly, Yasuda, Schuetz

Wrote or contributed to the writing of the manuscript: Ganguly, Yasuda, Schuetz

Downloaded from dmd.aspetjournals.org at ASPET Journals on April 23, 2024

DMD Fast Forward. Published on August 15, 2018 as DOI: 10.1124/dmd.118.083584
This article has not been copyedited and formatted. The final version may differ from this version.

REFERENCES

Ahmed-Belkacem A, Pozza A, Munoz-Martinez F, Bates SE, Castanys S, Gamarro F, Di Pietro A, and Perez-Victoria JM (2005) Flavonoid structure-activity studies identify 6-prenylchrysin and tectochrysin as potent and specific inhibitors of breast cancer resistance protein ABCG2. *Cancer Res* **65:**4852-4860.

Allen JD, Brinkhuis RF, Wijnholds J, and Schinkel AH (1999) The mouse Bcrp1/Mxr/Abcp gene: amplification and overexpression in cell lines selected for resistance to topotecan, mitoxantrone, or doxorubicin. *Cancer Res* **59:**4237-4241.

Almela L, Fernandez-Lopez JA, and Roca MJ (2000) High-performance liquid chromatographic screening of chlorophyll derivatives produced during fruit storage. *J Chromatogr A* **870:**483-489.

Bakhsheshian J, Hall MD, Robey RW, Herrmann MA, Chen JQ, Bates SE, and Gottesman MM (2013) Overlapping substrate and inhibitor specificity of human and murine ABCG2. *Drug Metab Dispos* **41:**1805-1812.

Dahan A and Amidon GL (2010) MRP2 mediated drug-drug interaction: indomethacin increases sulfasalazine absorption in the small intestine, potentially decreasing its colonic targeting. *Int J Pharm* **386:**216-220.

Di Gion P, Kanefendt F, Lindauer A, Scheffler M, Doroshyenko O, Fuhr U, Wolf J, and Jaehde U (2011) Clinical pharmacokinetics of tyrosine kinase inhibitors: focus on pyrimidines, pyridines and pyrroles. *Clin Pharmacokinet* **50:**551-603.

Ellis LC, Hawksworth GM, and Weaver RJ (2013) ATP-dependent transport of statins by human and rat MRP2/Mrp2. *Toxicol Appl Pharmacol* **269:**187-194.

Downloaded from dmd.aspetjournals.org at ASPET Journals on April 23, 2024

DMD Fast Forward. Published on August 15, 2018 as DOI: 10.1124/dmd.118.083584
This article has not been copyedited and formatted. The final version may differ from this version.

Giacomini KM, Huang SM, Tweedie DJ, Benet LZ, Brouwer KL, Chu X, Dahlin A, Evers R, Fischer V, Hillgren KM, Hoffmaster KA, Ishikawa T, Keppler D, Kim RB, Lee CA, Niemi M, Polli JW, Sugiyama Y, Swaan PW, Ware JA, Wright SH, Yee SW, Zamek-Gliszczynski MJ, and Zhang L (2010) Membrane transporters in drug development. *Nat Rev Drug Discov* **9:**215-236.

Gutmann H, Hruz P, Zimmermann C, Beglinger C, and Drewe J (2005) Distribution of breast cancer resistance protein (BCRP/ABCG2) mRNA expression along the human GI tract. *Biochem Pharmacol* **70:**695-699.

Hu S, Chen Z, Franke R, Orwick S, Zhao M, Rudek MA, Sparreboom A, and Baker SD (2009) Interaction of the multikinase inhibitors sorafenib and sunitinib with solute carriers and ATP-binding cassette transporters. *Clin Cancer Res* **15:**6062-6069.

Hudachek SF and Gustafson DL (2013) Incorporation of ABCB1-mediated transport into a physiologically-based pharmacokinetic model of docetaxel in mice. *J Pharmacokinet Pharmacodyn* **40:**437-449.

Inoue Y, Izawa K, Kiryu S, Tojo A, and Ohtomo K (2008) Diet and abdominal autofluorescence detected by in vivo fluorescence imaging of living mice. *Mol Imaging* **7:**21-27.

Jonker JW, Buitelaar M, Wagenaar E, Van Der Valk MA, Scheffer GL, Scheper RJ, Plosch T, Kuipers F, Elferink RP, Rosing H, Beijnen JH, and Schinkel AH (2002) The breast cancer resistance protein protects against a major chlorophyll-derived dietary phototoxin and protoporphyria. *Proc Natl Acad Sci U S A* **99:**15649-15654.

Kamath AV, Wang J, Lee FY, and Marathe PH (2008) Preclinical pharmacokinetics and in vitro metabolism of dasatinib (BMS-354825): a potent oral multi-targeted kinase inhibitor against SRC and BCR-ABL. *Cancer Chemother Pharmacol* **61:**365-376.

Downloaded from dmd.aspetjournals.org at ASPET Journals on April 23, 2024

DMD Fast Forward. Published on August 15, 2018 as DOI: 10.1124/dmd.118.083584
This article has not been copyedited and formatted. The final version may differ from this version.

Kraatz M, Whitehead TR, Cotta MA, Berhow MA, and Rasmussen MA (2014) Effects of Chlorophyll-Derived Efflux Pump Inhibitor Pheophorbide a and Pyropheophorbide a on Growth and Macrolide Antibiotic Resistance of Indicator and Anaerobic Swine Manure Bacteria. *International Journal of Antibiotics* **2014:**14.

Krishnamurthy P and Schuetz JD (2006) Role of ABCG2/BCRP in biology and medicine. *Annu Rev Pharmacol Toxicol* **46:**381-410.

Kusuhara H, Furuie H, Inano A, Sunagawa A, Yamada S, Wu C, Fukizawa S, Morimoto N, Ieiri I, Morishita M, Sumita K, Mayahara H, Fujita T, Maeda K, and Sugiyama Y (2012) Pharmacokinetic interaction study of sulphasalazine in healthy subjects and the impact of curcumin as an in vivo inhibitor of BCRP. *Br J Pharmacol* **166:**1793-1803.

Lagas JS, van Waterschoot RA, Sparidans RW, Wagenaar E, Beijnen JH, and Schinkel AH (2010) Breast cancer resistance protein and P-glycoprotein limit sorafenib brain accumulation. *Mol Cancer Ther* **9:**319-326.

Leblond F, Davis SC, Valdes PA, and Pogue BW (2010) Pre-clinical whole-body fluorescence imaging: Review of instruments, methods and applications. *J Photochem Photobiol B* **98:**77-94.

Lee CA, O'Connor MA, Ritchie TK, Galetin A, Cook JA, Ragueneau-Majlessi I, Ellens H, Feng B, Taub ME, Paine MF, Polli JW, Ware JA, and Zamek-Gliszczynski MJ (2015) Breast cancer resistance protein (ABCG2) in clinical pharmacokinetics and drug interactions: practical recommendations for clinical victim and perpetrator drug-drug interaction study design. *Drug Metab Dispos* **43:**490-509.

Downloaded from dmd.aspetjournals.org at ASPET Journals on April 23, 2024

DMD Fast Forward. Published on August 15, 2018 as DOI: 10.1124/dmd.118.083584
This article has not been copyedited and formatted. The final version may differ from this version.

Mahringer A, Delzer J, and Fricker G (2009) A fluorescence-based in vitro assay for drug interactions with breast cancer resistance protein (BCRP, ABCG2). *Eur J Pharm Biopharm* **72:**605-613.

Mao Q and Unadkat JD (2015) Role of the breast cancer resistance protein (BCRP/ABCG2) in drug transport--an update. *AAPS J* **17:**65-82.

McConnell EL, Basit AW, and Murdan S (2008) Measurements of rat and mouse gastrointestinal pH, fluid and lymphoid tissue, and implications for in-vivo experiments. *J Pharm Pharmacol* **60:**63-70.

Pavek P, Merino G, Wagenaar E, Bolscher E, Novotna M, Jonker JW, and Schinkel AH (2005) Human breast cancer resistance protein: interactions with steroid drugs, hormones, the dietary carcinogen 2-amino-1-methyl-6-phenylimidazo(4,5-b)pyridine, and transport of cimetidine. *J Pharmacol Exp Ther* **312:**144-152.

Polli JW, Humphreys JE, Harmon KA, Castellino S, O'Mara MJ, Olson KL, John-Williams LS, Koch KM, and Serabjit-Singh CJ (2008) The role of efflux and uptake transporters in [N-{3-chloro-4-[(3-fluorobenzyl)oxy]phenyl}-6-[5-({[2-(methylsulfonyl)ethyl]amino }methyl)-2-furyl]-4-quinazolinamine (GW572016, lapatinib) disposition and drug interactions. *Drug Metab Dispos* **36:**695-701.

Roberts JK, Birg AV, Lin T, Daryani VM, Panetta JC, Broniscer A, Robinson GW, Gajjar AJ, and Stewart CF (2016) Population Pharmacokinetics of Oral Topotecan in Infants and Very Young Children with Brain Tumors Demonstrates a Role of ABCG2 rs4148157 on the Absorption Rate Constant. *Drug Metab Dispos* **44:**1116-1122.

Downloaded from dmd.aspetjournals.org at ASPET Journals on April 23, 2024

DMD Fast Forward. Published on August 15, 2018 as DOI: 10.1124/dmd.118.083584
This article has not been copyedited and formatted. The final version may differ from this version.

Robey RW, Steadman K, Polgar O, and Bates SE (2005) ABCG2-mediated transport of photosensitizers: potential impact on photodynamic therapy. *Cancer Biol Ther* **4:**187-194.

Robey RW, Steadman K, Polgar O, Morisaki K, Blayney M, Mistry P, and Bates SE (2004) Pheophorbide a is a specific probe for ABCG2 function and inhibition. *Cancer Res* **64:**1242-1246.

Robey RW, To KK, Polgar O, Dohse M, Fetsch P, Dean M, and Bates SE (2009) ABCG2: a perspective. *Adv Drug Deliv Rev* **61:**3-13.

Sane R, Agarwal S, and Elmquist WF (2012) Brain distribution and bioavailability of elacridar after different routes of administration in the mouse. *Drug Metab Dispos* **40:**1612-1619.

Schwabedissen HEMz and Kroemer HK (2011) In Vitro and In Vivo Evidence for the Importance of Breast Cancer Resistance Protein Transporters (BCRP/MXR/ABCP/ABCG2), in: *Drug Transporters* (Fromm MF and Kim RB eds), pp 325-371, Springer Berlin Heidelberg, Berlin, Heidelberg.

Strumberg D, Clark JW, Awada A, Moore MJ, Richly H, Hendlisz A, Hirte HW, Eder JP, Lenz HJ, and Schwartz B (2007) Safety, pharmacokinetics, and preliminary antitumor activity of sorafenib: a review of four phase I trials in patients with advanced refractory solid tumors. *Oncologist* **12:**426-437.

Suzuki K, Doki K, Homma M, Tamaki H, Hori S, Ohtani H, Sawada Y, and Kohda Y (2009) Co-administration of proton pump inhibitors delays elimination of plasma methotrexate in high-dose methotrexate therapy. *Br J Clin Pharmacol* **67:**44-49.

Downloaded from dmd.aspetjournals.org at ASPET Journals on April 23, 2024

DMD Fast Forward. Published on August 15, 2018 as DOI: 10.1124/dmd.118.083584
This article has not been copyedited and formatted. The final version may differ from this version.

Tweedie D, Polli JW, Berglund EG, Huang SM, Zhang L, Poirier A, Chu X, and Feng B (2013) Transporter studies in drug development: experience to date and follow-up on decision trees from the International Transporter Consortium. *Clin Pharmacol Ther* **94:**113-125.

US Food and Drug Administration-Center for Drug Evaluation and Research (2017a)Guidance for Industry: Clinical Drug Interaction Studies — Study Design, Data Analysis, and Clinical Implications Guidance for Industry. *FDA, Maryland.* https://www.fda.gov/downloads/drugs/guidances/ucm292362.pdf

US Food and Drug Administration-Center for Drug Evaluation and Research (2017b) Guidance for Industry: In Vitro Metabolism and Transporter Mediated Drug-Drug Interaction Studies. *FDA , Maryland.* https://www.fda.gov/downloads/Drugs/Guidances/UCM581965.pdf

Weiss J, Rose J, Storch CH, Ketabi-Kiyanvash N, Sauer A, Haefeli WE, and Efferth T (2007) Modulation of human BCRP (ABCG2) activity by anti-HIV drugs. *J Antimicrob Chemother* **59:**238-245.

Zhang W, Li J, Allen SM, Weiskircher EA, Huang Y, George RA, Fong RG, Owen A, and Hidalgo IJ (2009) Silencing the breast cancer resistance protein expression and function in caco-2 cells using lentiviral vector-based short hairpin RNA. *Drug Metab Dispos* **37:**737-744.

Zhongfa L, Chiu M, Wang J, Chen W, Yen W, Fan-Havard P, Yee LD, and Chan KK (2012) Enhancement of curcumin oral absorption and pharmacokinetics of curcuminoids and curcumin metabolites in mice. *Cancer Chemother Pharmacol* **69:**679-689.

Downloaded from dmd.aspetjournals.org at ASPET Journals on April 23, 2024

DMD Fast Forward. Published on August 15, 2018 as DOI: 10.1124/dmd.118.083584
This article has not been copyedited and formatted. The final version may differ from this version.

FOOTNOTES

Samit Ganguly and Kazuto Yasuda contributed equally to this work.

The work was supported by the National Cancer Institute [Cancer Center Support Grant P30 CA21765]; and the American Lebanese Syrian Associated Charities (ALSAC).

Downloaded from dmd.aspetjournals.org at ASPET Journals on April 23, 2024

DMD Fast Forward. Published on August 15, 2018 as DOI: 10.1124/dmd.118.083584
This article has not been copyedited and formatted. The final version may differ from this version.

FIGURE LEGENDS

Figure 1. Autofluorescence derived from dietary PhA is higher in the Bcrp KO compared to WT mice. Comparison of fluorescence (Ex675/Em840) in WT and Bcrp KO mice fed a regular diet or AFF diet at least for three days (A). Comparison of fluorescence (Ex675/Em840) in a regular and AFF diet (B). Fluorescence comparison of known concentrations of chlorophyll a (CLPa), PhA and a prototypical Bcrp substrate protoporphyrin IX (PPIX) fluorescence with filter setting (Ex675/Em840) (C).

Figure 2. Absence of Bcrp leads to higher absorption of PhA in enterocytes. *Ex vivo* image comparison of intestinal segments of WT and Bcrp KO mice on a regular diet, after flushing out the gut contents with saline (A). Microscopic examination of cross-sectional images of upper intestine from WT and Bcrp KO mice on regular diet; blue is Dapi stain for nuclear localization) and red is Pheophorbide A using the Cyanine5 Ex/Em wavelengths.

Figure 3. PhA oral absorption is significantly higher in the Bcrp KO mice. Representative image comparing of PhA fluorescence (Ex675/Em840) in WT and Bcrp KO mice, 2 hrs after oral administration of 10 mg/kg PhA (A). Fluorescence intensity over zero- hour WT fluorescence-time profile up to 6 hours following 10 mg/kg of PhA oral administration in Bcrp WT and KO mice (n=3) (B). Comparison of Area under the fluorescence ratio time curve up to 6 hrs ($AUC_{FL\ 0\text{-}6h}$) in Figure B calculated using GraphPad Prism v5.02 (C). Comparison of PhA serum concentration at 1, 2,4 and 6 hrs from the WT and Bcrp KO mice dosed 10 mg/kg PhA

Downloaded from dmd.aspetjournals.org at ASPET Journals on April 23, 2024

DMD Fast Forward. Published on August 15, 2018 as DOI: 10.1124/dmd.118.083584
This article has not been copyedited and formatted. The final version may differ from this version.

(D) and the associated $AUC_{Serum\ 0\text{-}6h}$ (E). Results are presented as means ± SEM; and significance is calculated at $p < 0.05$ by comparing the means with unpaired t-test. *** $P < 0.001$.

Figure 4. Determination of the IC_{50} for selected Bcrp inhibitors using PhA as a probe substrate. Mean % increase in Pheophorbide A accumulation ± SEM in the MDCKII cells overexpressing BCRP in the presence of selected Bcrp inhibitors was plotted against the log transformed inhibitor concentration. IC_{50} was determined using GraphPad Prism v5.02.

Figure 5. Inhibition of BCRP increased whole body fluorescence as well as the serum concentration of PhA in control FVB mice. Six hour representative image comparing fluorescence (Ex675/Em840) in control mice orally administrated 10 mg/kg of PhA ± Bcrp inhibitors, 1 hr prior to PhA administration as indicated in the methods (A). Whole body fluorescence (flux/sec) was normalized to the zero-hour fluorescence of the same mice and data plotted as mean fluorescence ratio ± SEM vs. time (hrs), for the tyrosine kinase inhibitors (B) and other inhibitors (C). $AUC_{FL\ 0\text{-}6h}$ calculated for each mouse and plotted as mean ± SEM (D). PhA serum concentration- time plot for the control and tyrosine kinase inhibitors (E) and other inhibitors (F) plotted as mean ±SEM and the associated $AUC_{Serum\ 0\text{-}6h}$ calculated using GraphPad Prism v5.02 (G). Significance is calculated by comparing the mean AUC after inhibitor treatment with that of control AUC by unpaired t-test. Significance is calculated at $p<0.05$. * $p<0.05$, ** $p<0.01$, *** $p<0.001$.

Downloaded from dmd.aspetjournals.org at ASPET Journals on April 23, 2024

DMD Fast Forward. Published on August 15, 2018 as DOI: 10.1124/dmd.118.083584
This article has not been copyedited and formatted. The final version may differ from this version.

Table 1. Literature reported properties of selected inhibitors and final outcome of the experiment

		DSB	SFB	PPZ	ECD	CCM	LPB
Known parameters from literature and database	Mol. Wt. (gm/mol)	488.01	464.83	383.37	563.65	368.38	581.06
	Pred. Sol. (μM) (DrugBank)	26.23	3.68	1291.18	4.99	15.61	38.38
	Pred. logP (DrugBank)	2.77	4.12	2.11	6.81	3.62	5.18
	Reported IC_{50} (μM)		3.1[1]	5.5[2]	0.31[3]	1.6[4]	0.025[5]
Clinical information	Dose	100 mg OD[6]	400 mg BID	40 mg SD [7]	400 mg BID [7]	2 gm SD [7]	1250 mg QD [7]
	C_{max} (μM)	0.46[6]	6.45 [8]	6.5 [7]	0.327 [7]		4.2 [7]
	I_{gut}/IC_{50}		1110	67 [7]	9200 [7]	14000 [7]	210000 [7]
	C_{max}/IC_{50}		2.08	1.2 [7]	1.1 [7]		170 [7]
	Possible DDI	No	Yes	Yes	Yes	Yes	Yes
PK information from mice	Dose (mg/kg)	10	40	40	100	300	90
	C_{max} (μM)	~ 0.7 [11]	21 [1]		0.78 [9]	~0.06 [13]	~ 10 [12]
	T_{max} (h)	0.25- 2	1 [10]		8	1.5	0.5-1
	$T_{1/2}$ (h)				20	12	3
Prediction of possible outcome in mouse based on selected dose and observed IC_{50}	Observed IC_{50} (μM)	22.76	2.18	11.19	0.21	2.52	0.04
	C_{max}/ IC_{50}	0.03	9.63		3.71	0.02	250
	Oral Dose for mice study (mg/kg)	10	40	40	100	300	90
	C_{gut} (μM)	639	2689	3260	5544	25449	4840
	C_{gut}/ IC_{50}	28	1233	291	26400	10098	121000
	$C_{gut\_soluble}$/ IC_{50}	1.2	1.7	115.4	23.7	6.2	959.5
	Expected Oral DDI	Yes	Yes	Yes	Yes	Yes	Yes
***In vivo* serum concentration result**	$AUC_{Serum\ 0\text{-}6h}$ (μM·h)	0.11 ± 0.002	0.13 ± 0.02	0.18 ± 0.01	0.46 ± 0.08	0.70 ± 0.1	1.24 ± 0.09
	Fold Change over control	1.24	1.45	2.02	5.17	7.79	13.78
	Observed DDI?	No	No	Yes	Yes	Yes	Yes
Live animal fluorescence result	$AUC_{FL\ 0\text{-}6h}$	5.82 ± 1.27	6.98 ± 1.15	7.30 ± 0.74	10.55 ± 2.12	11.2 ± 1.75	11.66 ± 1.54
	Fold Change over control	1.2	1.44	1.50	2.17	2.31	2.4
	Observed DDI?	No	No	Yes	Yes	Yes	Yes

Notes: Mol. Wt. = molecular weight; Pred. Sol = Predicted aqueous solubility; I_{gut} = Clinical dose / 250 mL; C_{gut} = mouse dose / 0.8 mL (mouse gut fluid volume); $C_{gut\_soluble}$ = Pred. Solubility

[1](Hu et al., 2009); [2] (Suzuki et al., 2009); [3](Ahmed-Belkacem et al., 2005); [4](Kusuhara et al., 2012); [5](Polli et al., 2008); [6](Di Gion et al., 2011); [7](Lee et al., 2015); [8](Strumberg et al., 2007); [9](Sane et al., 2012); [10](Lagas et al., 2010); [11](Kamath et al., 2008); [12](Hudachek and Gustafson, 2013); [13](Zhongfa et al., 2012)

Downloaded from dmd.aspetjournals.org at ASPET Journals on April 23, 2024

DMD Fast Forward. Published on August 15, 2018 as DOI: 10.1124/dmd.118.083584
This article has not been copyedited and formatted. The final version may differ from this version.

FIGURES

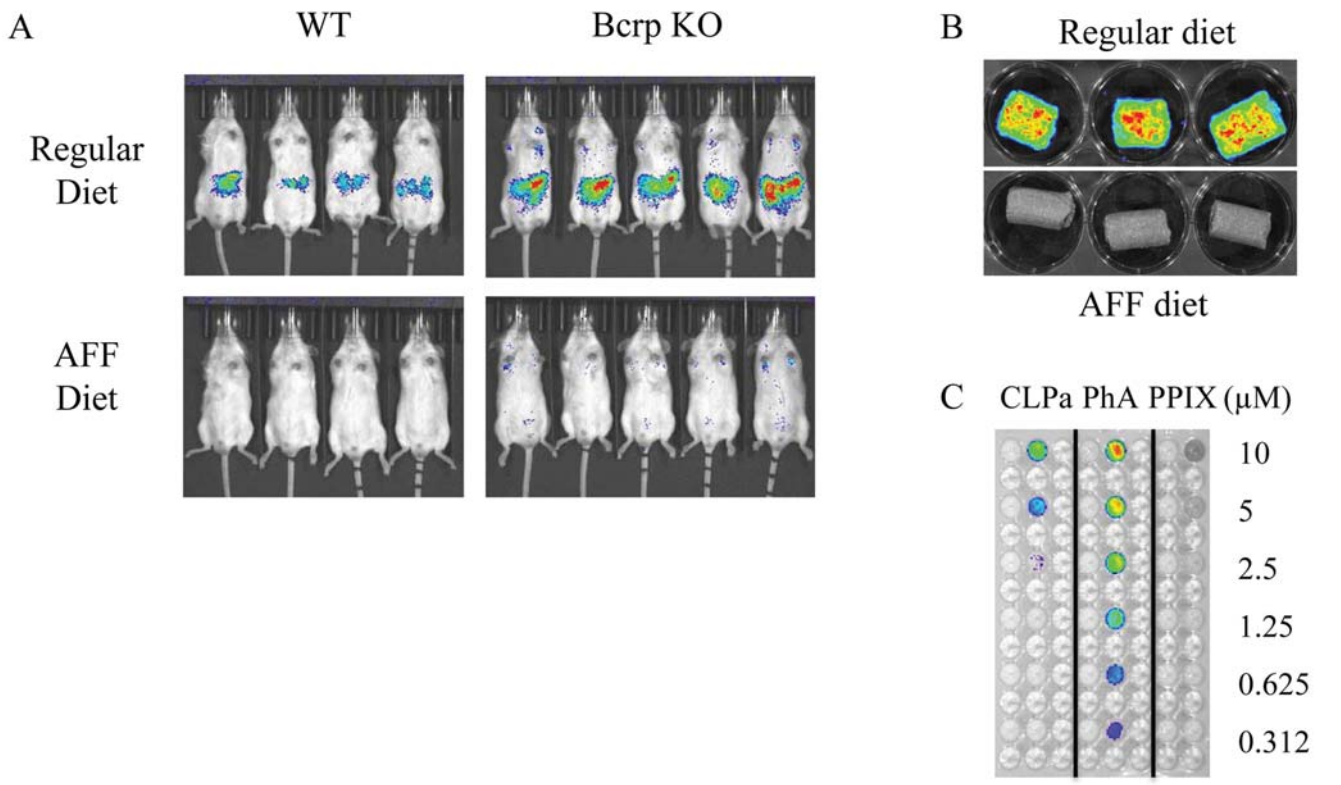

Figure 1

Downloaded from dmd.aspetjournals.org at ASPET Journals on April 23, 2024

DMD Fast Forward. Published on August 15, 2018 as DOI: 10.1124/dmd.118.083584
This article has not been copyedited and formatted. The final version may differ from this version.

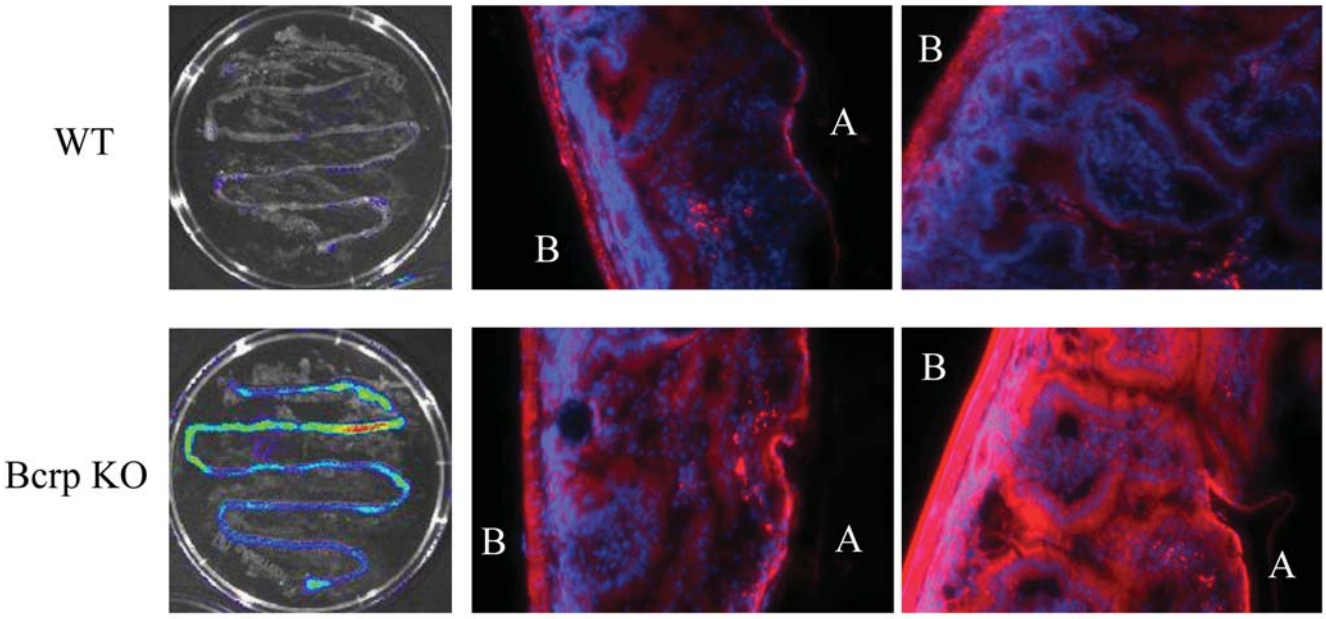

Figure 2

Downloaded from dmd.aspetjournals.org at ASPET Journals on April 23, 2024

DMD Fast Forward. Published on August 15, 2018 as DOI: 10.1124/dmd.118.083584
This article has not been copyedited and formatted. The final version may differ from this version.

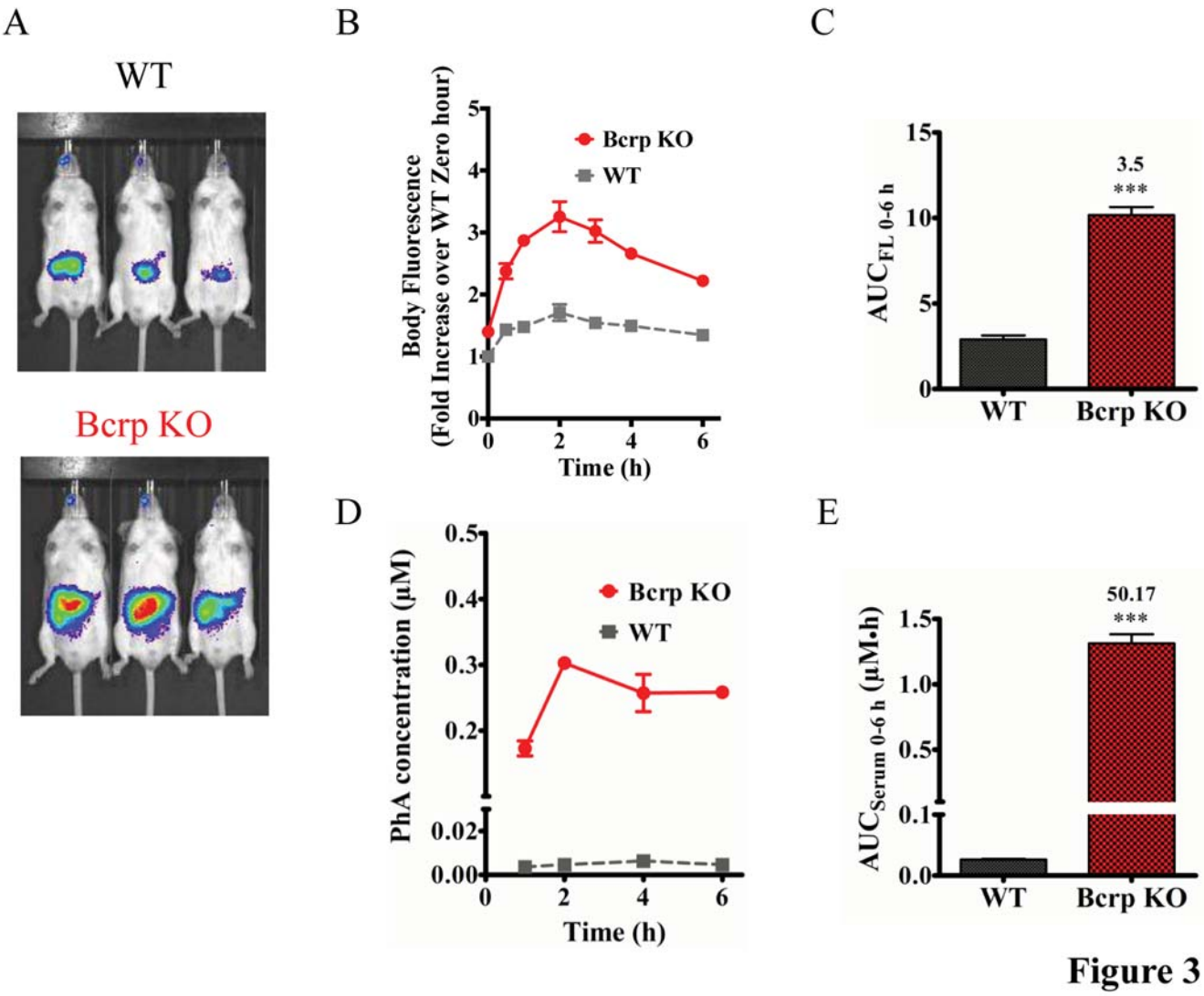

Figure 3

Downloaded from dmd.aspetjournals.org at ASPET Journals on April 23, 2024

DMD Fast Forward. Published on August 15, 2018 as DOI: 10.1124/dmd.118.083584
This article has not been copyedited and formatted. The final version may differ from this version.

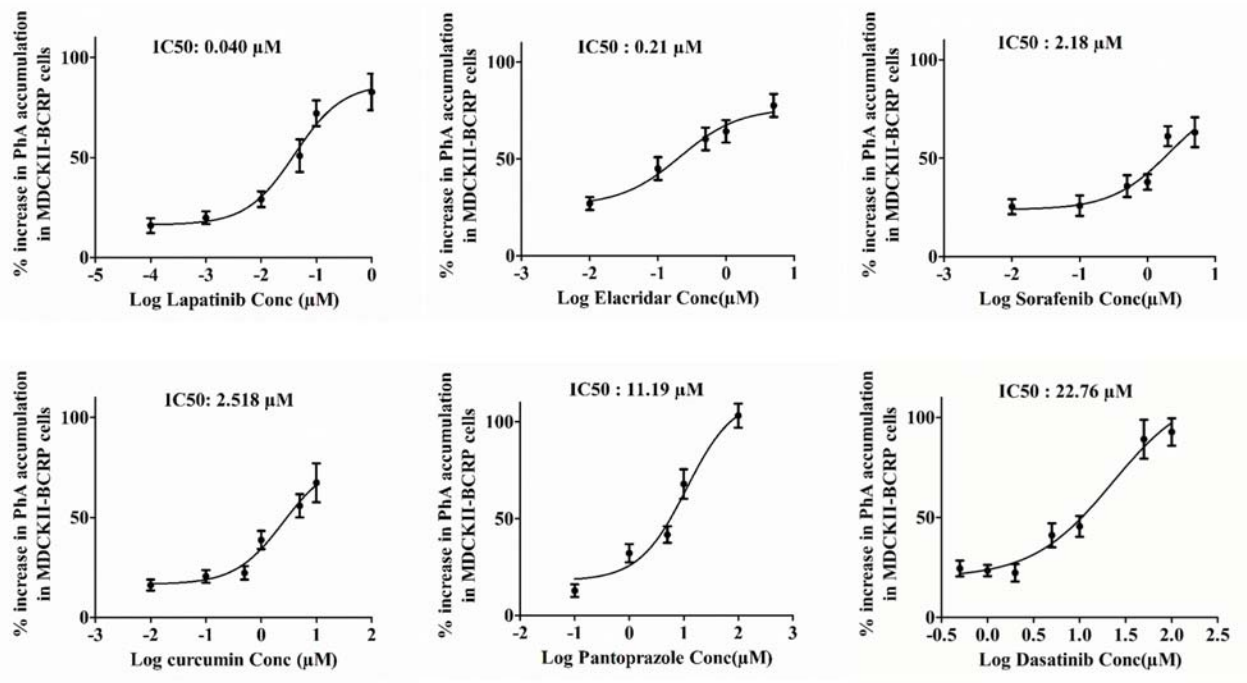

Figure 4

Downloaded from dmd.aspetjournals.org at ASPET Journals on April 23, 2024

DMD Fast Forward. Published on August 15, 2018 as DOI: 10.1124/dmd.118.083584
This article has not been copyedited and formatted. The final version may differ from this version.

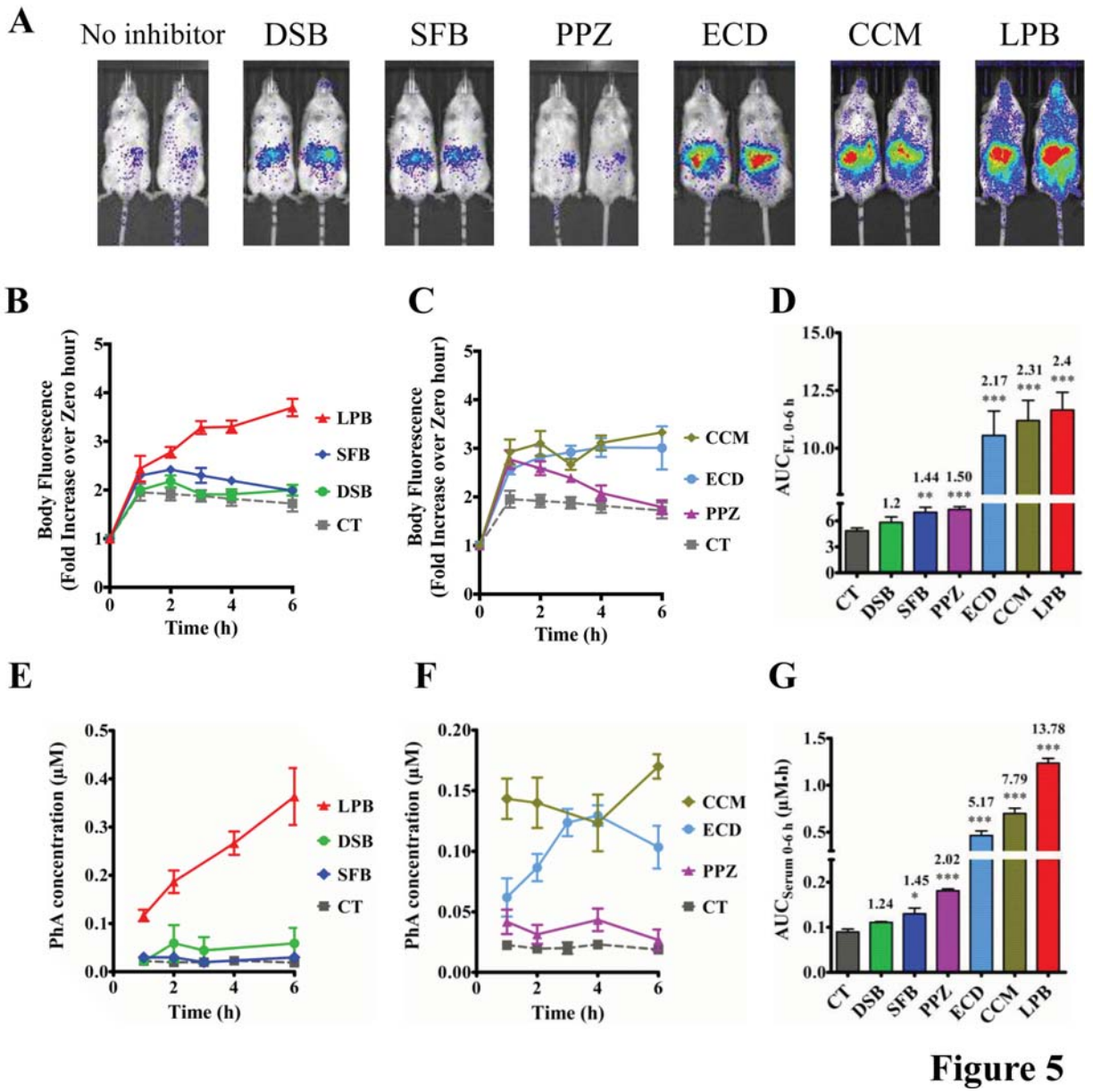

Figure 5

Downloaded from dmd.aspetjournals.org at ASPET Journals on April 23, 2024